



Coordination polymers constructed by diverse metal centers and the rigid ligand 3,5-di(1*H*-imidazol-1-yl)pyridine: Synthesis, structure and properties

Li Luo^a, Yue Zhao^a, Yi Lu^a, Taka-aki Okamura^b, Wei-Yin Sun^{a,*}

^aCoordination Chemistry Institute, State Key Laboratory of Coordination Chemistry, School of Chemistry and Chemical Engineering, Nanjing National Laboratory of Microstructures, Nanjing University, Nanjing 210093, China

^bDepartment of Macromolecular Science, Graduate School of Science, Osaka University, Toyonaka, Osaka 560-0043, Japan

ARTICLE INFO

Article history:

Received 22 November 2011

Accepted 13 February 2012

Available online 3 March 2012

Keywords:

Coordination polymers

3,5-Di(1*H*-imidazol-1-yl)pyridine

Anion exchange

Photoluminescence property

ABSTRACT

Six new coordination polymers, [Cu(L)₂(H₂O)₂](NO₃)₂ (**1**), [Cu(L)₂(ClO₄)₂] (**2**), [Cd(L)₂(H₂O)₂](ClO₄)₂ (**3**), [Cd(L)(OAc)₂(H₂O)] (**4**), [Cu₃(L)₄(H₂O)₂(SO₄)](SO₄)₂·30H₂O (**5**), and [Ni(L)(H₂O)₃(SO₄)] (**6**) [L = 3,5-di(1*H*-imidazol-1-yl)pyridine, OAc[−] = CH₃COO[−]], have been prepared and characterized by X-ray diffraction, IR, elemental and thermogravimetric analyses. Complexes **1**, **4** and **6** have different one-dimensional (1D) chain structures, while **2** and **4** are two-dimensional (2D) networks. The chains and layers are further linked together by hydrogen bonds to generate three-dimensional (3D) frameworks. Complex **5** is a (3,4,4)-connected 3D framework with a Point (Schläfli) symbol of (4.8²)₄(4.8³·10²)₂(4²·8²·10²). The influences of the coordination modes of the ligand L, metal center as well as the counteranion on the structures of the complexes are discussed. Furthermore, the reversible anion exchange property of **3** and the photoluminescence properties of **3** and **4** have been investigated.

© 2012 Elsevier Ltd. All rights reserved.

1. Introduction

In recent years, metal–organic frameworks (MOFs) have attracted great attention from chemists, not only due to their intriguing structures [1] but also because of their potential applications in gas storage, optics, ion exchange, separation, catalysis and so on [2–7]. However, it is still a challenge to predict and exactly control the compositions and structures of the complexes [8]. Employing multidentate organic ligands and metal ions to construct inorganic–organic hybrid materials through metal–ligand coordination and hydrogen bonding interactions has become a major strategy. In previously reported works, rigid or flexible tripodal ligands such as 2,4,6-tris(4-pyridyl)-1,3,5-triazine, 1,3,5-tris(1-imidazolyl)benzene and 1,3,5-tris(imidazol-1-ylmethyl)benzene have been well used to prepare complexes with varied metal salts [9–11]. For example, metal complexes with different structures and properties have been obtained by the reactions of the 1,3,5-tris(imidazol-1-ylmethyl)benzene ligand with a variety of metal salts, such as CuSO₄·5H₂O, MnSO₄·H₂O, CdSO₄·8/3H₂O and Cu(ClO₄)₂·6H₂O [10,11]. The results show that many factors, such as the coordination geometry of metal center, the counteranion, the coordination mode of the ligand, the ratio of metal salt to ligand, the reaction medium and temperature can influence the structure of the complexes. This attracted us to carry out further studies to understand the impact of the assembly process.

We focused our attention on the constructions, structures and properties of MOFs with imidazole-containing organic ligands [12]. Given that the coordination abilities of the N atom of pyridine and imidazole groups have subtle differences, in this work we designed a new ligand, 3,5-di(1*H*-imidazol-1-yl)pyridine (L), which includes both pyridine and imidazole groups. Herein, we report the preparations and crystal structures of six new complexes, [Cu(L)₂(H₂O)₂](NO₃)₂ (**1**), [Cu(L)₂(ClO₄)₂] (**2**), [Cd(L)₂(H₂O)₂](ClO₄)₂ (**3**), [Cd(L)(OAc)₂(H₂O)] (**4**), [Cu₃(L)₄(H₂O)₂(SO₄)](SO₄)₂·30H₂O (**5**) and [Ni(L)(H₂O)₃(SO₄)] (**6**). The thermal stability, photoluminescence and anion exchange properties of the complexes have been investigated.

2. Experimental

2.1. Materials and measurements

All commercially available chemicals and solvents are of reagent grade and were used as received without further purification. Elemental analyses for C, H and N were performed on a Perkin-Elmer 240C Elemental Analyzer at the analysis center of Nanjing University. Thermogravimetric analyses (TGA) were performed on a simultaneous SDT 2960 thermal analyzer under nitrogen, with a heating rate of 10 °C min^{−1}. FT-IR spectra were recorded in the range 400–4000 cm^{−1} on a Bruker Vector22 FT-IR spectrophotometer using KBr pellets. X-ray powder diffraction (XRPD) patterns were obtained on a Shimadzu XRD-6000 X-ray diffractometer with Cu Kα (λ = 1.5418 Å) radiation at room temperature. The

* Corresponding author. Tel.: +86 25 83593485; fax: +86 25 83314502.

E-mail address: sunwy@nju.edu.cn (W.-Y. Sun).

luminescence spectra for the powdered solid samples were measured on an Aminco Bowman Series 2 spectrofluorometer with a xenon arc lamp as the light source. In the measurements of emission and excitation spectra, the pass width was 5 nm, and all the measurements were carried out under the same experimental conditions.

2.2. Synthesis of the ligand L

The title compound was prepared by a similar procedure reported for the preparation of 1,3,5-tris(1-imidazolyl)benzene using 3,5-dibromopyridine instead of 1,3,5-tribromobenzene [13]. 3,5-Dibromopyridine (2.84 g, 12.0 mmol), imidazole (3.26 g, 48.0 mmol), K_2CO_3 (4.42 g, 32.0 mmol) and anhydrous $CuSO_4$ (0.05 g, 0.31 mmol) were mixed well and heated at 180 °C for 12 h under a nitrogen atmosphere. The mixture was cooled to room temperature and washed with water. The residue was dissolved in boiling water, filtered while hot and left to crystallize, to give the ligand L in 86% yield. 1H NMR [$(CD_3)_2SO$] δ (ppm): 8.97 (s, 2H), 8.50 (s, 2H), 8.48 (s, 1H), 7.98 (s, 2H), 7.21 (s, 2H); *Anal. Calc.* for $C_{11}H_9N_5$: C, 62.55; H, 4.29; N, 33.16. Found: C, 62.74; H, 4.18; N, 33.04%.

2.3. Synthesis of $[Cu(L)_2(H_2O)_2](NO_3)_2$ (**1**)

The title complex was prepared by the layering method. A buffer layer of a CH_3OH/H_2O (1:1) solution (8 mL) was carefully layered over a solution of L (10.5 mg, 0.05 mmol) in H_2O (3 mL). Then a solution of $Cu(NO_3)_2 \cdot 3H_2O$ (12.5 mg, 0.05 mmol) in CH_3OH (3 mL) was layered over the buffer layer. Block blue crystals were obtained after 2 weeks in 82% yield. *Anal. Calc.* for $C_{22}H_{22}N_{12}O_8Cu$: C, 40.90; H, 3.43; N, 26.02. Found: C, 40.95; H, 3.44; N, 25.97%. IR (KBr pellet, cm^{-1}): 3393 (m), 1604 (m), 1512 (s), 1455 (w), 1398 (s), 1355 (s), 1326 (s), 1255 (m), 1127 (w), 1077 (m), 999 (w), 863 (w), 770 (w), 740 (m), 685 (m), 664 (m).

2.4. Synthesis of $[Cu(L)_2](ClO_4)_2$ (**2**)

This complex was obtained by the same procedure used for the preparation of **1**, except that $Cu(ClO_4)_2 \cdot 6H_2O$ (18.6 mg, 0.05 mmol) instead of $Cu(NO_3)_2 \cdot 3H_2O$ was used as the starting material. Purple platelet crystals were obtained in 75% yield after 1 month. *Anal. Calc.* for $C_{22}H_{18}Cl_2N_{10}O_8Cu$: C, 38.58; H, 2.65; N, 20.45. Found: C, 38.50; H, 2.64; N, 20.49%. IR (KBr pellet, cm^{-1}): 3405 (w), 1602 (m), 1522 (s), 1463 (w), 1323 (w), 1272 (m), 1081 (s), 950 (m), 899 (m), 825 (m), 736 (m), 693 (m), 642 (m), 619 (s).

2.5. Synthesis of $[Cd(L)_2(H_2O)_2](ClO_4)_2$ (**3**)

This complex was obtained by the same procedure used for the preparation of **2**, except that $Cd(ClO_4)_2 \cdot 6H_2O$ (20.1 mg, 0.05 mmol) instead of $Cu(ClO_4)_2 \cdot 6H_2O$ was used as the starting material. Colorless block crystals were obtained in 85% yield after 2 weeks. *Anal. Calc.* for $C_{22}H_{22}Cl_2N_{10}O_{10}Cd$: C, 34.33; H, 2.88; N, 18.20. Found: C, 34.26; H, 2.87; N, 18.23%. IR (KBr pellet, cm^{-1}): 3464 (m), 2923 (w), 1604 (m), 1497 (s), 1326 (w), 1291 (w), 1248 (s), 1085 (s), 928 (w), 891 (w), 827 (m), 777 (w), 693 (w), 621 (m).

2.6. Synthesis of $[Cd(L)(OAc)_2(H_2O)]$ (**4**)

This complex was obtained by the same procedure used for the preparation of **3**, except that $Cd(OAc)_2 \cdot 2H_2O$ (13.3 mg, 0.05 mmol) instead of $Cd(ClO_4)_2 \cdot 6H_2O$ was used as the starting material. Colorless platelet crystals were obtained in 80% yield after 2 weeks. The crystals were collected by filtration. *Anal. Calc.* for $C_{15}H_{17}N_5O_5Cd$: C, 39.19; H, 3.73; N, 15.23. Found: C, 39.24; H, 3.72; N, 15.20%. IR (KBr pellet, cm^{-1}): 3243 (w), 3122 (m), 1576 (s), 1497 (s), 1405

(s), 1313 (s), 1256 (m), 1120 (w), 1070 (m), 1006 (w), 921 (w), 757 (m), 671 (m), 643 (m).

2.7. Synthesis of $[Cu_3(L)_4(H_2O)_2(SO_4)](SO_4)_2 \cdot 30H_2O$ (**5**)

The complex was obtained by the same procedure used for the preparation of **1**, except that $CuSO_4 \cdot 5H_2O$ (12.5 mg, 0.05 mmol) instead of $Cu(NO_3)_2 \cdot 3H_2O$ was used as the starting material. Blue block crystals were obtained in 90% yield after 2 weeks. *Anal. Calc.* for $C_{44}H_{102}N_{20}O_{45}S_3Cu_3$: C, 27.55; H, 5.36; N, 14.60. Found: C, 27.50; H, 5.37; N, 14.57%. IR (KBr pellet, cm^{-1}): 3390 (m), 3120 (m), 1609 (m), 1514 (s), 1272 (m), 1126 (s), 964 (w), 854 (w), 774 (w), 685 (w), 613 (m).

2.8. Synthesis of $[Ni(L)(H_2O)_3(SO_4)]$ (**6**)

This complex was obtained by the same procedure used for the preparation of **5**, except that $NiSO_4 \cdot 6H_2O$ (13.1 mg, 0.05 mmol) instead of $CuSO_4 \cdot 5H_2O$ was used as the starting material. Blue-green block crystals were obtained in 87% yield after 2 weeks. *Anal. Calc.* for $C_{11}H_{15}N_5O_7Ni$: C, 31.45; H, 3.60; N, 16.67. Found: C, 31.39; H, 3.61; N, 16.64%. IR (KBr pellet, cm^{-1}): 3252 (m), 1683 (w), 1602 (m), 1522 (s), 1272 (s), 1170 (s), 1096 (s), 1052 (s), 958 (m), 884 (w), 825 (w), 723 (m), 649 (m), 576 (m).

2.9. Procedure for reversible anion exchange of complex **3**

A well-ground powder of the complex $[Cd(L)_2(H_2O)_2](ClO_4)_2$ (**3**) (60 mg) was suspended in a water (5 mL) solution of $NaNO_3$ (1.0 g), and the mixture was well stirred for 1 day at room temperature, then the solid was collected by centrifuging, washed with water several times, and eventually dried in a vacuum to give the anion exchanged product $[Cd(L)_2(H_2O)_2](NO_3)_2$ (**3A**). *Anal. Calc.* for **3A** ($C_{22}H_{22}N_{12}O_8Cd$): C, 38.03; H, 3.19; N, 24.19. Found: C, 37.97; H, 3.18; N, 24.23%. To investigate the reversibility of such an anion exchange, the anion exchanged solid **3A** was suspended in an aqueous solution (5 mL) of $NaClO_4$ (1.0 g). The mixture was stirred for 1 day at room temperature, and then handled by the same procedure described above, and the anion exchanged sample $[Cd(L)_2(H_2O)_2](ClO_4)_2$ (**3B**) was obtained. *Anal. Calc.* for **3B** ($C_{22}H_{22}Cl_2N_{10}O_{10}Cd$): C, 34.33; H, 2.88; N, 18.20. Found: C, 34.28; H, 2.87; N, 18.21%.

2.10. X-ray crystallography

The X-ray diffraction measurements for complexes **2**, **5** and **6** were made on a Rigaku Rapid II imaging plate area detector with Mo $K\alpha$ radiation ($\lambda = 0.71075 \text{ \AA}$) using a MicroMax-007HF micro-focus rotating anode X-ray generator and a VariMax-Mo optics at 200 K. The structures of **2**, **5** and **6** were solved by direct methods with SIR92 [14] and expanded using Fourier techniques with DIRFID-99 [15]. The non-hydrogen atoms were refined anisotropically by the full matrix least-squares method on F^2 . The hydrogen atoms of coordinated water molecules in **6** were located from the Fourier map, while the ones of the uncoordinated water molecules in **5** were not found. The hydrogen atoms of the ligand L were generated geometrically and refined isotropically using the riding model. All calculations of **2**, **5** and **6** were performed using the CrystalStructure [16] crystallographic software package, except for refinement which was performed using SHELXL-97 [17]. The crystallographic data collections for **1**, **3** and **4** were carried out on a Bruker Smart Apex CCD with graphite-monochromated Mo $K\alpha$ radiation ($\lambda = 0.71073 \text{ \AA}$) at 293(2) K using the ω -scan technique. The data were integrated using the SAINT program [18], which was also used for the intensity corrections for Lorentz and polarization effects. A semi-empirical absorption correction was applied using the SADABS program [19]. The structures were solved by direct methods and

Table 1
Crystal data and structure refinements for complexes **1–6**.

Compound	1	2	3
Empirical formula	C ₂₂ H ₂₂ N ₁₂ O ₈ Cu	C ₂₂ H ₁₈ Cl ₂ N ₁₀ O ₈ Cu	C ₂₂ H ₂₂ Cl ₂ N ₁₀ O ₁₀ Cd
Formula weight	646.07	684.90	769.80
Crystal system	triclinic	monoclinic	monoclinic
Space group	<i>P</i> $\bar{1}$	<i>P</i> 2 ₁ / <i>c</i>	<i>P</i> 2 ₁ / <i>n</i>
<i>a</i> (Å)	8.119(2)	10.429(4)	8.9190(16)
<i>b</i> (Å)	9.100(3)	9.147(2)	10.5618(19)
<i>c</i> (Å)	10.427(3)	16.235(5)	15.241(3)
α (°)	114.069(4)	90.00	90.00
β (°)	108.807(5)	127.659(15)	98.550(3)
γ (°)	92.394(5)	90.00	90.00
<i>T</i> (K)	293	200	293
<i>V</i> (Å ³)	652.3(3)	1226.1(7)	1419.8(4)
<i>Z</i>	1	2	2
<i>D</i> _{calc} (g cm ⁻³)	1.645	1.855	1.801
μ (mm ⁻¹)	0.911	1.184	1.032
<i>F</i> (000)	331.00	694.00	772
θ for data collection (°)	2.5–25.10	3.17–27.48	2.35–25.10
Reflections collected	3278	11279	6890
Unique reflections	2264	2807	2529
Goodness-of-fit	1.228	1.136	1.056
<i>R</i> ₁ ^a , <i>wR</i> ₂ ^b [<i>I</i> > 2 σ (<i>I</i>)]	0.0689, 0.1418	0.0332, 0.0890	0.0686, 0.1450
<i>R</i> ₁ , <i>wR</i> ₂ (all data)	0.0753, 0.1447	0.0366, 0.0907	0.0721, 0.1469
Compound	4	5	6
Empirical formula	C ₁₅ H ₁₇ N ₅ O ₅ Cd	C ₄₄ H ₁₀₂ N ₂₀ O ₄₅ S ₃ Cu ₃	C ₁₁ H ₁₅ N ₅ O ₇ SNi
Formula weight	459.75	1918.26	420.05
Crystal system	monoclinic	monoclinic	monoclinic
Space group	<i>C</i> 2/ <i>c</i>	<i>P</i> 2 ₁ / <i>c</i>	<i>P</i> 2 ₁ / <i>c</i>
<i>a</i> (Å)	11.8243(8)	12.6148(18)	7.5823(17)
<i>b</i> (Å)	17.7204(12)	10.9249(19)	11.145(3)
<i>c</i> (Å)	8.4141(6)	32.348(5)	17.811(6)
α (°)	90.00	90.00	90.00
β (°)	96.2970(10)	112.180(7)	102.875(14)
γ (°)	90.00	90.00	90.00
<i>T</i> (K)	293(2)	200	200
<i>V</i> (Å ³)	1752.4(2)	4128.2(11)	1467.2(7)
<i>Z</i>	4	2	4
<i>D</i> _{calc} (g cm ⁻³)	1.743	1.543	1.902
μ (mm ⁻¹)	1.282	0.948	1.517
<i>F</i> (000)	920	2002.00	864.00
θ for data collection (°)	2.08–25.09	3.19–25.00	3.20–27.49
Reflections collected	4404	27375	13061
Unique reflections	1566	7186	3332
Goodness-of-fit	1.026	1.052	1.127
<i>R</i> ₁ ^a , <i>wR</i> ₂ ^b [<i>I</i> > 2 σ (<i>I</i>)]	0.0212, 0.0494	0.0662, 0.1844	0.0335, 0.0842
<i>R</i> ₁ , <i>wR</i> ₂ (all data)	0.0226, 0.0501	0.0756, 0.1923	0.0355, 0.0850

^a $R_1 = \sum ||F_o| - |F_c|| / \sum |F_o|$.

^b $wR_2 = [\sum w(|F_o|^2 - |F_c|^2)] / [\sum w(F_o^2)]^{1/2}$, where $w = 1 / [\sigma^2(F_o^2) + (aP)^2 + bP]$, $P = (F_o^2 + 2F_c^2) / 3$.

all non-hydrogen atoms were refined anisotropically on *F*² by the full-matrix least-squares technique using the SHELXL crystallographic software package [20]. The hydrogen atoms of coordinated water molecules in **1**, **3** and **4** were located from the Fourier map and all the other hydrogen atoms were generated geometrically and refined isotropically using the riding model. Details of the crystal parameters, data collection and refinements for the complexes are summarized in Table 1, and selected bond lengths and angles are listed in Table 2.

3. Results and discussion

3.1. Crystal structural description of [Cu(L)₂(H₂O)₂](NO₃)₂ (**1**)

The coordination environment around the Cu(II) atom is shown in Fig. 1a, along with the atom numbering scheme. Cu1 is six-coordinated with a distorted octahedral coordination geometry by four N atoms (N52, N52D, N32B, N32C) from four distinct L ligands, with Cu1–N bond distances of 2.011(4) and 2.026(4) Å, and two O atoms from two coordinated water molecules with a Cu1–O bond length

of 2.446 Å [21], and the bond angles around Cu1 are in the range 86.6(1)–180°. Each L ligand links two Cu(II) atoms using its two imidazole groups, while the pyridine group of the ligand L does not participate in the coordination (Scheme 1a). Such a coordination mode makes **1** an infinite one-dimensional (1D) hinged chain structure (Fig. 1b). The adjacent chains are further held together through O–H...N and O–H...O hydrogen bonding interactions, generating a two-dimensional (2D) network (Fig. S1a). The layers are then linked by C–H...O hydrogen bonds to give rise to the final three-dimensional (3D) framework structure (Fig. S1b). The hydrogen bonding data of **1–6** are provided in the Supporting information (Table S1).

3.2. Crystal structural description of [Cu(L)₂](ClO₄)₂ (**2**)

In order to investigate the effect of the counteranion on the structure of the complexes, the reaction using Cu(ClO₄)₂·6H₂O was carried out under the same reaction conditions as for the synthesis of **1**, and fortunately complex **2**, with a different structure, was obtained. The crystal structure of **2** is shown in Fig. 2a, each

Table 2
Selected bond lengths (Å) and angles (°) for complexes **1–6**.^a

Compound 1					
Cu(1)–N(52)	2.011(4)	Cu(1)–N(32)#1	2.026(4)	Cu(1)–O(1)	2.446(4)
N(52)–Cu(1)–N(32)	87.6(2)	N(52)#2–Cu(1)–N(32)#3	92.4(2)	N(52)–Cu(1)–O(1)	88.4(2)
N(52)#2–Cu(1)–O(1)	91.6(2)	N(32)#3–Cu(1)–O(1)	86.6(1)	N(32)#1–Cu(1)–O(1)	93.4(1)
Compound 2					
Cu(1)–N(32)	1.995(2)	Cu(1)–N(52)#1	2.011(2)		
N(32)#2–Cu(1)–N(52)#1	91.31(6)	N(32)–Cu(1)–N(52)#1	88.69(6)		
Compound 3					
Cd(1)–N(52)	2.307(5)	Cd(1)–O(5)	2.311(5)	Cd(1)–N(32)#1	2.342(5)
N(52)#2–Cd(1)–O(5)#2	92.8(2)	N(52)–Cd(1)–O(5)#2	87.2(2)	O(5)#2–Cd(1)–N(32)#1	94.6(2)
O(5)–Cd(1)–N(32)#1	85.4(2)	N(52)#2–Cd(1)–N(32)#1	92.0(2)	N(52)–Cd(1)–N(32)#1	88.0(2)
Compound 4					
Cd(1)–N(3)	2.307(2)	Cd(1)–O(1)	2.405(2)	Cd(1)–O(5)	2.291(3)
Cd(1)–O(2)	2.476(2)				
O(1)–Cd(1)–O(2)	53.09(6)	N3#1–Cd(1)–N(3)	176.52(9)	N(3)–Cd(1)–O(2)#1	91.42(6)
N(3)#1–Cd(1)–O(1)	90.99(7)	N(3)–Cd(1)–O(5)	88.26(4)	N(3)#1–Cd(1)–O(2)#1	91.29(6)
N(3)–Cd(1)–O(1)	88.87(7)	O(1)–Cd(1)–O(5)	87.78(4)	O(1)#1–Cd(1)–O(1)	175.56(8)
O(2)–Cd(1)–O(5)	140.87(4)	O(1)–Cd(1)–O(2)#1	131.34(6)	O(2)–Cd(1)–O(2)#1	78.26(8)
Compound 5					
Cu(1)–N(32)#1	2.023(4)	Cu(1)–O(9)	2.447(4)	Cu(1)–N(152)	2.019(4)
Cu(2)–O(1)	2.179(3)	Cu(2)–N(1)	2.045(3)	Cu(2)–N(52)#1	1.985(4)
Cu(2)–N(101)#2	2.030(3)	Cu(2)–N(132)	2.003(3)		
N(32)#1–Cu(1)–N(152)	92.2(2)	N(32)#3–Cu(1)–N(152)	87.8(2)	O(1)–Cu(2)–N(1)	97.1(1)
O(1)–Cu(2)–N(52)#1	97.0(2)	O(1)–Cu(2)–N(101)#2	96.4(2)	N(52)#1–Cu(2)–N(132)	91.8(2)
N(52)#1–Cu(2)–N(101)#2	166.6(1)	O(1)–Cu(2)–N(132)	96.6(2)	N(1)–Cu(2)–N(52)#1	87.8(2)
N(1)–Cu(2)–N(132)	166.2(1)	N(132)–Cu(2)–N(101)#2	86.4(2)	N(1)–Cu(2)–N(101)#2	90.9(1)
Compound 6					
Ni(1)–O(1)	2.084(1)	Ni(1)–O(2)	2.107(1)	Ni(1)–O(3)	2.054(1)
Ni(1)–O(11)	2.082(1)	Ni(1)–N(1)#1	2.135(2)	Ni(1)–N(32)	2.051(2)
O(1)–Ni(1)–O(2)	177.66(6)	O(1)–Ni(1)–O(3)	94.19(6)	O(1)–Ni(1)–O(11)	87.05(6)
O(1)–Ni(1)–N(1)#1	90.29(6)	O(1)–Ni(1)–N(32)	91.29(6)	O(2)–Ni(1)–N(32)	89.16(6)
O(3)–Ni(1)–N(32)	90.48(6)	O(11)–Ni(1)–N(32)	91.67(6)	O(11)–Ni(1)–N(1)#1	91.11(6)
O(3)–Ni(1)–N(1)#1	86.71(6)	O(2)–Ni(1)–O(3)	88.10(6)	O(2)–Ni(1)–O(11)	90.63(6)
O(2)–Ni(1)–N(1)#1	89.37(6)	N(1)#1–Ni(1)–N(32)	176.87(6)	O(3)–Ni(1)–O(11)	177.49(6)

^a Symmetry operators: #1: 1 + x, y, 1 + z; #2: 2 – x, –y, 2 – z; #3: 1 – x, –y, 1 – z for **1**; #1: –X + 2, Y – 1/2, –Z + 3/2; #2: –X + 2, –Y + 1, –Z + 1 for **2**; 1#: 1/2 – x, 1/2 + y, 2 – z; 2#: 1 – x, 2 – y, –z for **3**; #1: –x, y, –1/2 – z for **4**; #1: –X + 1, Y + 1/2, –Z + 1/2; #2: –X + 2, Y – 1/2, –Z + 1/2; #3: X + 1, –Y + 1/2, Z + 1/2; #4: –X + 1, Y – 1/2, –Z + 1/2; #5: –X + 2, –Y + 1, –Z + 1 for **5**; #1: X, –Y + 3/2, Z – 1/2 for **6**.

asymmetric unit of **2** contains one Cu(II) atom sitting on an inversion center, one L ligand and one perchlorate anion. The Cu1 atom

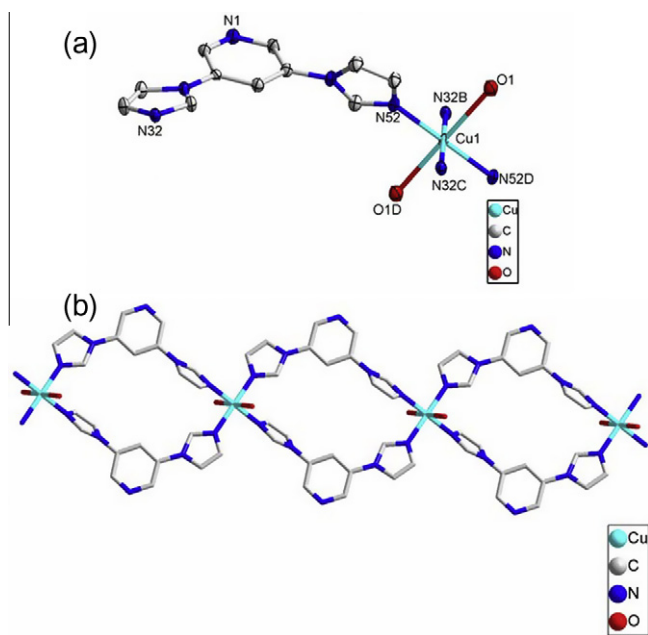
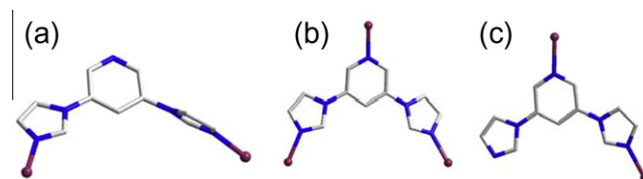


Fig. 1. (a) Coordination environment of the Cu(II) atom in complex **1** with the ellipsoids drawn at the 30% probability level. The hydrogen atoms and nitrate anion are omitted for clarity. (b) The infinite hinged chain structure of complex **1**.

is four coordinated with a nearly ideal square planar coordination geometry by four N atoms (N32, N32F, N52C, N52G) from four different L ligands, with N–Cu1–N bond angles in the range 88.69(6)–180° and Cu1–N bond lengths of 1.995(2) and 2.011(2) Å (Table 2). The coordination mode of L in **2** is similar to that in **1** (Scheme 1a), however, a layer structure, rather than the chain structure of **1**, is observed in **2** (Fig. 2b). Four L ligands and four Cu(II) atoms form a 40-membered macrocycle, which is further linked by Cu–N coordinated bonds to generate a 2D net with (4, 4) topology. The layers of **2** are packing along the c axis and the perchlorate anions are located in the voids (Fig. 2c). The layers are then linked by C–H...O hydrogen bonds to form the final 3D framework structure (Fig. S2).

3.3. Crystal structural description of [Cd(L)₂(H₂O)₂](ClO₄)₂ (**3**)

When Cd(ClO₄)₂·6H₂O was reacted with the ligand L to see the effect of the metal center on the structure, complex **3** was obtained. As illustrated in Fig. 3a, Cd1 in **3** has a distorted octahedral coordination geometry, six-coordinated with an N₄O₂ donor set.



Scheme 1. Coordination modes of the ligand L in complexes **1–6**.

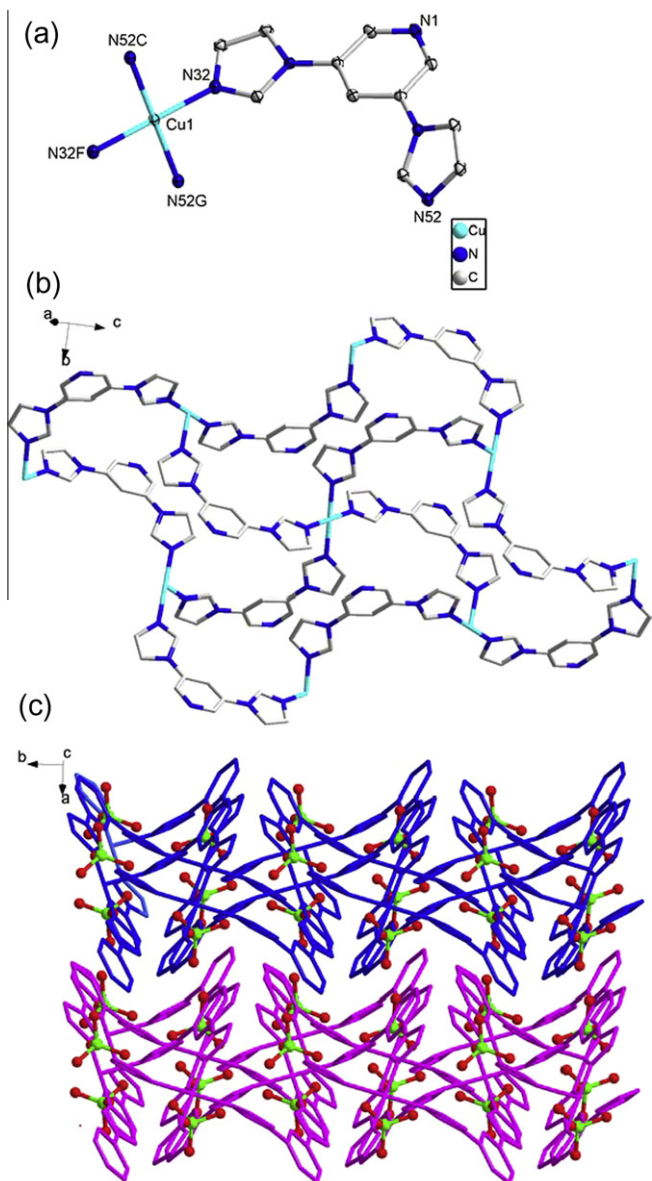


Fig. 2. (a) Coordination environment of the Cu(II) atom in complex **2** with the ellipsoids drawn at the 30% probability level. The hydrogen atoms and perchlorate anion are omitted for clarity. (b) The 2D network in complex **2** with (4, 4) topology. (c) Crystal packing diagram of complex **2** with perchlorate anions shown in the Ball and Stick mode and different colors for different layers. (Color online.)

The Cd–N bond distances are 2.307(5) and 2.342(5) Å and that of Cd–O is 2.311(5) Å. The range of bond angles is 85.4(2)–180.0° (Table 2). Due to the absence of the coordination of the pyridine group, the L ligand is a two-connector and links the Cd(II) centers to generate a 2D network structure (Fig. 3b), which is similar to that in **2**.

The layers of **3** are packed in an –ABAB– sequence along the *c* axis, and the perchlorate anions are located at the edge of the layers. There are O–H⋯N, O–H⋯O and C–H⋯O hydrogen bonds (Table S1) which link the layers and perchlorate anions to give rise to a 3D framework (Fig. S3).

3.4. Crystal structural description of [Cd(L)(OAc)₂(H₂O)] (**4**)

Considering that the nitrate and perchlorate anions in **1–3** do not take part in coordination with the metal centers, to investigate the

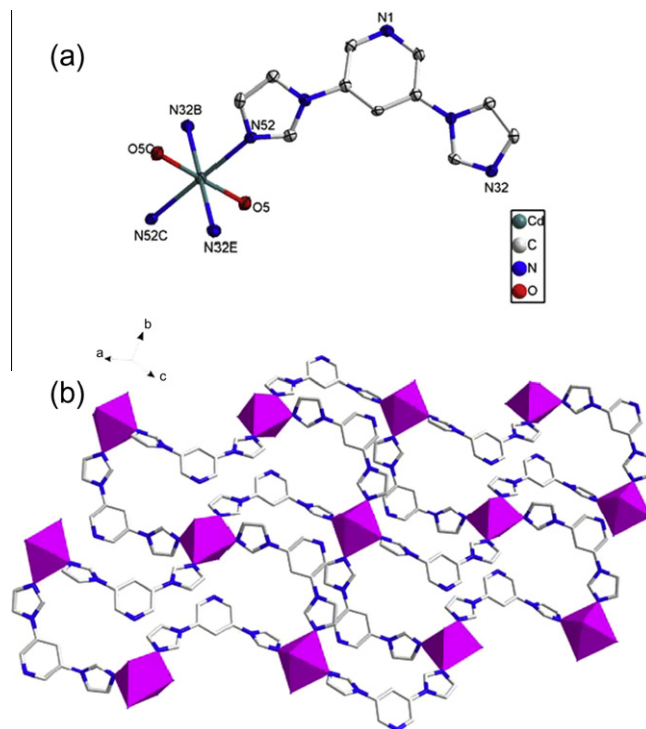


Fig. 3. (a) Coordination environment of the Cd(II) atom in complex **3** with the ellipsoids drawn at the 30% probability level. The hydrogen atoms and perchlorate anion are omitted for clarity. (b) The 2D network of complex **3**.

effect of counteranions with different coordination abilities on the structures of the complexes, the reaction of L with Cd(OAc)₂·2H₂O was carried out, and complex **4** was isolated. Each asymmetric unit of **4** contains one Cd(II) atom sitting on a special position, half L ligand and one acetate anion. As shown in Fig. 4a, the Cd1 atom is seven coordinated with a distorted pentagonal bipyramid coordination geometry, by two N atoms (N3, N3A) from the imidazole groups of two distinct L ligands with a Cd1–N bond distance of 2.307(2) Å, one O atom from water molecule with a Cd1–O5 bond distance of 2.291(3) Å and four O atoms from two acetate anions with Cd1–O bond lengths of 2.405(2) and 2.476(2) Å. The coordination angles around the Cd(II) center are in the range 53.09(6)–176.52(9)° (Table 2). On the other hand, each L ligand connects two Cd(II) atoms using its two imidazole groups to generate an infinite chain (Fig. 4b). The adjacent chains are further held together through O(5)–H(4)⋯O(1) and C(3)–H(3)⋯O(1) hydrogen bonding interactions, generating a 2D network (Fig. S4a). The layers are then linked together by C(1)–H(1)⋯O(2) hydrogen bonds to give rise to the final 3D framework structure (Fig. S4b).

3.5. Crystal structural description of [Cu₃(L)₄(H₂O)₂(SO₄)](SO₄)₂·30H₂O (**5**)

To compare with **1** and **2**, as well as to study the effect of a counteranion with a different charge and coordination ability on the structure of the complexes, the reaction of L with CuSO₄·5H₂O was carried out. As illustrated in Fig. 5a, there are two different Cu(II) atoms in the asymmetric unit of **5**. Each Cu1, sitting on an inversion center, is six-coordinated with a distorted octahedral coordination geometry by four N atoms (N32H, N152E, N32G, N152) from the imidazole groups of four distinct L ligands and two O atoms (O9, O9E) from water molecules. The Cu1–N bond lengths are 2.019(4) and 2.023(4) Å and the Cu1–O bond length is 2.447(4) Å (Table 2). While Cu2, with a distorted tetragonal pyra-

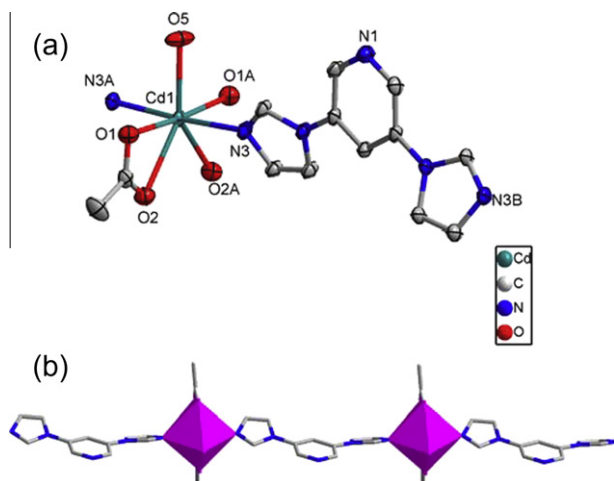


Fig. 4. (a) Coordination environment of the Cd(II) atom in complex **4** with the ellipsoids drawn at the 30% probability level. The hydrogen atoms are omitted for clarity. (b) The infinite chain structure of complex **4**.

midial coordination geometry, is five-coordinated by four N atoms (N1, N132, N101C, N52B) and one O atom from a sulfate anion. One of the N atoms is from the pyridine of one L ligand, and the others are from the imidazole groups of three other distinct L ligands. Thus, each Cu(II) atom in **5** links four L ligands. On the other hand, each L ligand connects three Cu(II) atoms using its pyridine and imidazole groups (Scheme 1b). If the coordination between Cu2 and N101 is neglected, the Cu(II) centers are bridged by L ligands to give rise to a 2D network in the *ab* plane, as illustrated in Fig. 5b. The layers are further linked together by Cu2–N101 bonds to generate a 3D framework with two different channels, A and B (Fig. 5c). The free sulfate anions occupy channel A along the *b*-axis, while the coordinated sulfate anions occupy channel B. The uncoordinated water molecules fill the vacancy of the 3D framework and are linked together via O–H...O hydrogen bonding interactions, though the hydrogen atoms of the uncoordinated water molecules in **5** could not be found.

To further understand the structure of **5**, a topological analysis by reducing the multi-dimensional structure to a simple node and linker net was carried out. The coordinated water molecules and sulfate anions are ignored in the topological analysis and each L ligand is a 3-connector, since one L ligand links three Cu(II) atoms. Each Cu(II) atom is attached to four L ligands, and thus can be regarded as a 4-connected node. The nodes corresponding to the L ligands are topologically equivalent while the Cu(II) nodes are different, therefore the overall structure of **5** is a (3,4,4)-connected trinodal 3D net, as shown in Fig. 5d, which is similar to the previously reported complex $[\text{Cu}_3(\text{trz})_4(\text{H}_2\text{O})_3]\text{F}_2$ ($\text{trz}^- = 1,2,4\text{-triazolate}$) with 3- and 4-connected nodes of *trz* and Cu(II), respectively [22]. The Point (Schläfli) symbol for the net is $(4.8^2)_4(4.8^3 \cdot 10^2)_2$ ($4^2 \cdot 8^2 \cdot 10^2$), calculated by the TOPOS program [23], and the name for the net is 3,4,4T24 [24].

3.6. Crystal structural description of $[\text{Ni}(\text{L})(\text{H}_2\text{O})_3(\text{SO}_4)]$ (**6**)

To further investigate the impact of the metal center on the structure of the complexes, $\text{NiSO}_4 \cdot 6\text{H}_2\text{O}$ was used in the reaction instead of $\text{CuSO}_4 \cdot 5\text{H}_2\text{O}$ to give complex **6**. It is interesting to find that one of the two imidazole groups, rather than the pyridine one as observed in **1–4**, does not participate in the coordination (Scheme 1c). As shown in Fig. 6a, in **6** each Ni(II) atom, with a distorted octahedral coordination geometry, is six-coordinated by three O atoms from three water molecules, one O from a sulfate anion, one N atom from the pyridine group of an L ligand and the

other N from the imidazole group of another L ligand. On the other hand, the L ligand links two Ni(II) atoms to generate an infinite zig-zag chain (Fig. 6b). The adjacent chains are joined together by O–H...O and O–H...N hydrogen bonds to give rise to a layer (Fig. S5a), which is further linked by O(1)–H(10)...O(14) and O(3)–H(15)...O(14) hydrogen bonds to generate the final 3D framework of **6** (Fig. S5b).

3.7. Comparison of the structures

Six coordination complexes of Cu(II), Cd(II) and Ni(II) were successfully obtained by the reactions of the rigid ligand L with the corresponding metal salts with different counteranions of NO_3^- , ClO_4^- and SO_4^{2-} under the same reaction conditions. The results show that the L ligand adopts three different coordination modes in **1–6** (Scheme 1). In the complexes **1–4**, each L ligand acts as a bidentate ligand using its two imidazole groups, with the pyridine group of L free of coordination (Scheme 1a). In **5**, the L ligand adopts a tridentate mode using its pyridine and two imidazole groups (Scheme 1b), while in **6**, the L ligand still adopts a bidentate mode, but using the pyridine and one of the imidazole groups (Scheme 1c). While compounds **1** and **2** have the same Cu(II) centers, they display different structures, namely **1** is an infinite chain, **2** is a 2D network. It can be seen that the distinct coordination number of the Cu(II) center results in the different structure, since the Cu(II) center is 6-coordinated in **1** and 4-coordinated in **2**. This phenomenon is also observed in complexes **3** and **4**. Comparing the structures of **3** and **4**, one more remarkable difference can be found, i.e. the OAc^- anion participates in coordination while the ClO_4^- anion does not take part in the coordination, which can be ascribed to the different coordination ability of the counteranions. Comparing complexes **5** and **6** with the same counteranion, the distinct structures can be brought about by the different coordination geometries of the metal centers as well as the different coordination mode of the L ligand (vide supra). The results further confirm that metal centers with different coordination numbers and geometries, counteranions with different coordination abilities and ligands with varied coordination modes play important roles in determining the structures of the complexes. At the same time, the present study implies that it is still a great challenge to control or foresee the overall structures of complexes at present since they can be influenced by subtle changes of factors such as metal center, counteranion and so on.

3.8. Thermal stabilities and XRPD of the complexes

Thermogravimetric analyses (TGA) were carried out for the complexes, except for **2** and **3** with perchlorate anions, and the results of the TGA are shown in Fig. S6. Complex **1** shows a weight loss of 5.08% before 165 °C, corresponding to the release of the coordinated water molecules (Calc. 5.18%), and further decomposition occurred at 320 °C. For **4**, the weight loss was found before 100 °C due to the release of the coordinated water molecules with a weight loss of 4.03% (Calc. 3.92%), and the decomposition temperature is 240 °C. For complex **5**, a weight loss of 26.1% was observed in the temperature range 30–170 °C, which corresponds to the release of water molecules, but it does not agree with the calculated value of 30.97%. The reason is that the solvent water molecules in **5** can be easily lost at room temperature. Complex **6** loses 12.70% of its weight in the temperature range 200–280 °C, which is attributed to the departure of the coordinated water molecules (Calc. 12.86%), and the residue is stable up to ca. 400 °C.

The purities of **1–6** were certified by X-ray powder diffraction (XRPD) measurements, and the results are given in Fig. S7. In addition, the diffraction patterns of **3A** and **3B** are shown in Fig. S8, which are in good agreement with that of **3**.

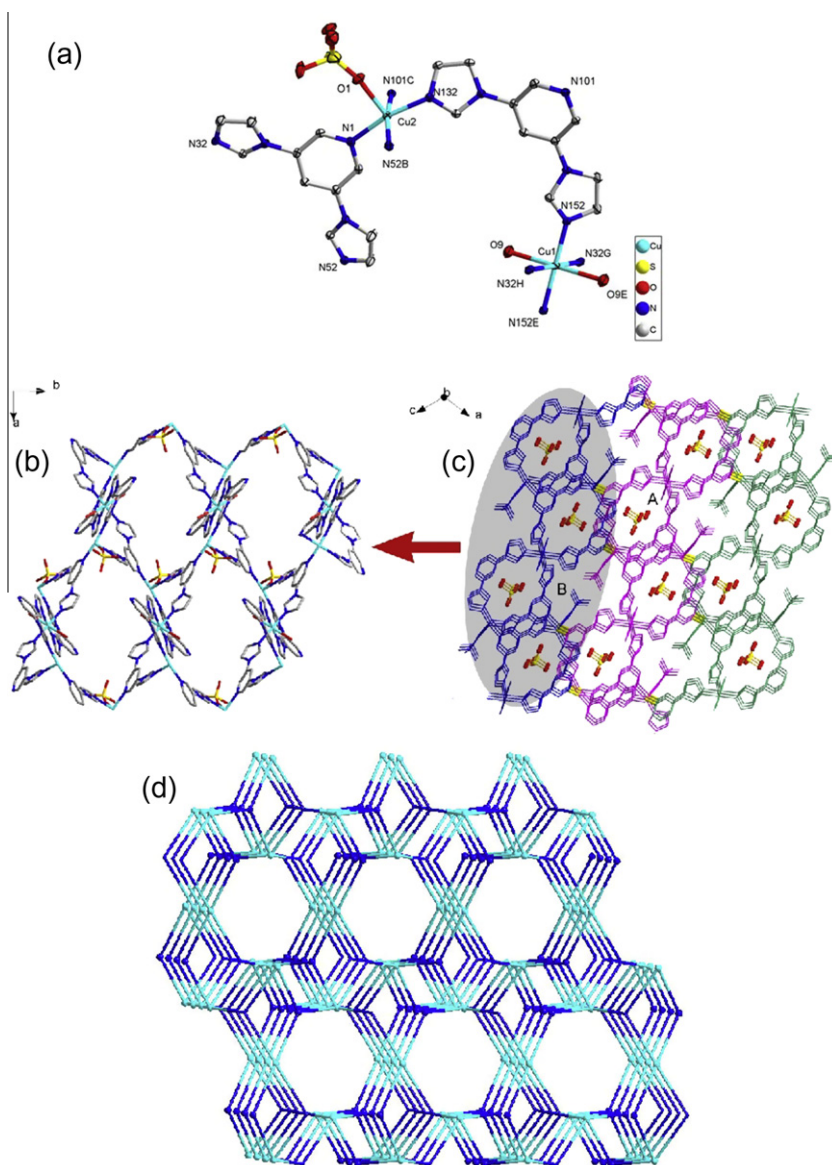


Fig. 5. (a) Coordination environment of the Cu(II) atoms in **5** with the ellipsoids drawn at the 30% probability level. The hydrogen atoms and uncoordinated sulfate anions are omitted for clarity. (b) The 2D network in **5**. (c) The 3D framework of **5** with different colors for different layers (yellow: Cu2–N101 bond). (d) The topological representation of the (3,4,4)-connected trinodal 3D structure of **5** with the $(4.8^2)_4(4.8^3 \cdot 10^2)_2(4^2 \cdot 8^2 \cdot 10^2)$ new topology (blue: Cu1 and Cu2; turquoise: L ligand). (Colour online.)

3.9. Reversible anion exchange property of complex **3**

The complex $[\text{Cd}(\text{L})_2(\text{H}_2\text{O})_2](\text{ClO}_4)_2$ (**3**) has a 2D network structure, and the perchlorate anions are located in the voids of the layers. Furthermore, **3** is insoluble in water and common organic solvents, thus anion exchange experiments were performed. The results show that **3** shows a reversible anion exchange property. A well-ground powder of **3** was suspended in an aqueous solution of NaNO_3 and stirred for 1 day, and then the exchanged product $[\text{Cd}(\text{L})_2(\text{H}_2\text{O})_2](\text{NO}_3)_2$ was obtained (see Section 2). The FT-IR spectra of **3** and the exchanged product are shown in Fig. 7. It can be seen that the intense bands at 1383 and 1312 cm^{-1} , originating from the NO_3^- anion, appear in the spectrum of **3A**, while the intense bands around 1132 and 1099 cm^{-1} of the ClO_4^- anion disappear. Furthermore, the results of the elemental analyses also confirm the complete anion exchange. Through the anion exchange of **3**, the framework structure is retained, which can be confirmed by the XRPD spectra of **3** and **3A** (Fig. S8). A powder sample of **3A** was suspended in an aqueous solution of NaClO_4 with constant

stirring for 1 day to allow the reverse anion exchange, and the product **3B** was obtained. The band of ClO_4^- appeared in the spectrum of **3B**, and the bands of NO_3^- disappeared (Fig. 7). The results indicate that **3** shows a reversible anion exchange property.

3.10. Photoluminescence of the complexes

The photoluminescence properties of the Cd(II) complexes have been well studied because of their potential application as fluorescence-emitting materials. The emission spectra of the Cd(II) complexes **3** and **4**, together with the free ligand L, were measured in the solid state at room temperature. Intense emission bands were observed at 398 nm for the free ligand L, with the excitation at 363 nm . As shown in Fig. S9, intense bands were observed at 397 nm ($\lambda_{\text{ex}} = 362\text{ nm}$) for **3** and 406 nm ($\lambda_{\text{ex}} = 353\text{ nm}$) for **4**. The emissions of **3** and **4** may tentatively be assigned to the intraligand transition of L as a result of their close similarity [25]. The small red shift of the emission maximum between the complex and the li-

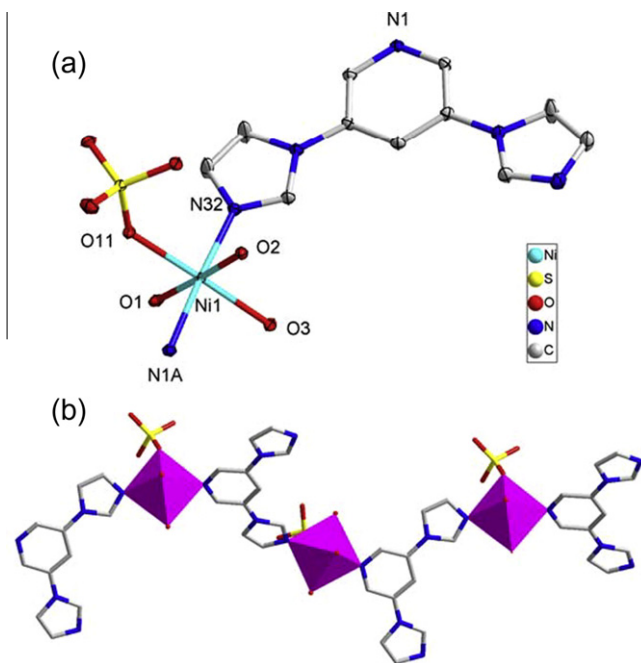


Fig. 6. (a) Coordination environment of the Ni(II) atom in complex **6** with the ellipsoids drawn at the 30% probability level. The hydrogen atoms are omitted for clarity. (b) The zigzag chain of complex **6**.

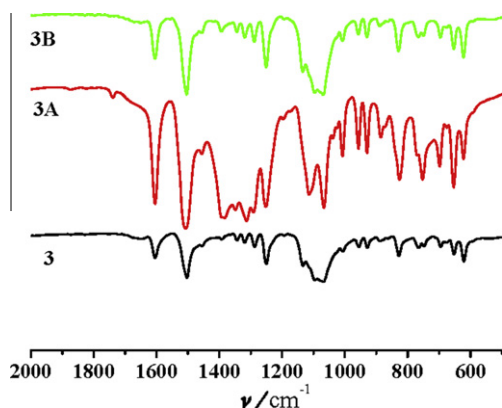


Fig. 7. IR spectra of **3**, exchanged product **3A** and reversed exchanged product **3B**.

gand L was considered to originate from the influence of the coordination of the ligand to the metal center.

4. Conclusion

The self-assembly of varied metal salts with the rigid imidazole-containing ligand 3,5-di(1*H*-imidazol-1-yl)pyridine results in the formation of six complexes with different structures. The results show that the counteranions with different charges, coordination ability and size, and metal centers with different coordination geometries have remarkable impact on the structures of the complexes. In addition, the diverse coordination modes of the ligands may also play an important role in the formation of the coordination polymers.

Acknowledgments

This work was financially supported by the National Natural Science Foundation of China (Grant Nos. 91122001 and

21021062) and the National Basic Research Program of China (Grant Nos. 2007CB925103 and 2010CB923303).

Appendix A. Supplementary data

CCDC 851230, 851231, 851232, 851233, 851234 and 851235 contain the supplementary crystallographic data for **1**, **2**, **3**, **4**, **5** and **6**. These data can be obtained free of charge via <http://www.ccdc.cam.ac.uk/conts/retrieving.html>, or from the Cambridge Crystallographic Data Centre, 12 Union Road, Cambridge CB2 1EZ, UK; fax: (+44) 1223-336-033; or e-mail: deposit@ccdc.cam.ac.uk. Supplementary data associated with this article can be found, in the online version, at [doi:10.1016/j.poly.2012.02.027](https://doi.org/10.1016/j.poly.2012.02.027).

References

- [1] (a) W.L. Meng, J. Fan, T. Okamura, H. Kawaguchi, Y. Lv, W.Y. Sun, N. Ueyama, *Z. Anorg. Allg. Chem.* 632 (2006) 1890; (b) S.Y. Zhang, S.Y. Yang, J.B. Lan, S.J. Yang, J.S. You, *Chem. Commun.* 46 (2008) 6170; (c) H.M. Guo, X. He, J.J. Liu, J. Han, M.X. Li, *Polyhedron* 30 (2011) 1982.
- [2] (a) B. Wang, A.P. Côté, H. Furukawa, M. O'Keeffe, O.M. Yaghi, *Nature* 453 (2008) 207; (b) Y.E. Cheon, M.P. Suh, *Angew. Chem., Int. Ed.* 48 (2009) 2899; (c) X. Lin, I. Telepeni, A.J. Blake, A. Dailly, C.M. Brown, J.M. Simmons, M. Zoppi, G.S. Walker, K.M. Thomas, T.J. Mays, P. Hubberstey, N.R. Champness, M. Schröder, *J. Am. Chem. Soc.* 131 (2009) 2159; (d) J.B. Lin, J.P. Zhang, X.M. Chen, *J. Am. Chem. Soc.* 132 (2010) 6654; (e) S.S. Chen, M. Chen, S. Takamizawa, M.S. Chen, Z. Su, W.Y. Sun, *Chem. Commun.* 47 (2011) 752; (f) M.S. Chen, M. Chen, S. Takamizawa, T. Okamura, J. Fan, W.Y. Sun, *Chem. Commun.* 47 (2011) 3787.
- [3] (a) X.M. Jiang, M.J. Zhang, H.Y. Zeng, G.C. Guo, J.S. Huang, *J. Am. Chem. Soc.* 133 (2011) 3410; (b) G.J. He, D. Guo, C. He, X.L. Zhang, X.W. Zhao, C.Y. Duan, *Angew. Chem., Int. Ed.* 48 (2009) 6312; (c) Z.Z. Lu, R. Zhang, Y.Z. Li, Z.J. Guo, H.G. Zheng, *J. Am. Chem. Soc.* 133 (2011) 4172.
- [4] (a) Q.Y. Yang, K. Li, J. Luo, M. Pan, C.Y. Su, *Chem. Commun.* 47 (2011) 4234; (b) G.C. Xu, Y.J. Ding, T. Okamura, Y.Q. Huang, Z.S. Bai, Q. Hua, G.X. Liu, W.Y. Sun, N. Ueyama, *Cryst. Growth Des.* 9 (2009) 395; (c) B.C. Tzeng, T.H. Chiu, B.S. Chen, G.H. Lee, *Chem. Eur. J.* 14 (2008) 5237.
- [5] (a) R. Banerjee, A. Phan, B. Wang, C. Knobler, H. Furukawa, M. O'Keeffe, O.M. Yaghi, *Science* 319 (2008) 939; (b) K. Li, D.H. Olson, J. Seidel, T.J. Emge, H. Gong, H. Zeng, J. Li, *J. Am. Chem. Soc.* 131 (2009) 10368.
- [6] (a) J.S. Seo, D. Whang, H. Lee, S.I. Jun, J. Oh, Y.J. Jeon, K. Kim, *Nature* 404 (2000) 982; (b) T. Tu, W. Assenmacher, H. Peterlik, G. Schnakenburg, K.H. Dötz, *Angew. Chem., Int. Ed.* 47 (2008) 7127; (c) S. Horike, M. Dinca, K. Tamaki, J.R. Long, *J. Am. Chem. Soc.* 130 (2008) 5854.
- [7] I. Imaz, R.M. Marta, G.F. Lorena, G. Francisca, R.M. Daniel, H. Jordi, P. Victor, M. Daniel, *Chem. Commun.* 46 (2010) 4737.
- [8] (a) B. Moulton, M.J. Zaworotko, *Chem. Rev.* 101 (2001) 1629; (b) E. Tynan, P. Jensen, P.E. Kruger, A.C. Lees, M. Nieuwenhuyzen, *J. Chem. Soc., Dalton Trans.* (2003) 1223.
- [9] (a) M. Yoshizawa, M. Tamura, M. Fujita, *Science* 312 (2006) 251; (b) B.Q. Ma, P. Coppens, *Chem. Commun.* (2004) 932.
- [10] J. Fan, B. Sui, T. Okamura, W.Y. Sun, N. Ueyama, *J. Chem. Soc., Dalton Trans.* (2002) 3868.
- [11] Z. Su, J. Fan, T. Okamura, M.S. Chen, S.S. Chen, W.Y. Sun, N. Ueyama, *Cryst. Growth Des.* 10 (2010) 1911.
- [12] (a) Z.P. Qi, Z.S. Bai, Q. Yuan, T. Okamura, K. Cai, Z. Su, W.Y. Sun, N. Ueyama, *Polyhedron* 27 (2008) 2672; (b) L.Y. Kong, Z.H. Zhang, H.F. Zhu, H. Kawaguchi, T. Okamura, M. Doi, Q. Chu, W.Y. Sun, N. Ueyama, *Angew. Chem., Int. Ed.* 44 (2005) 4352; (c) L.Y. Kong, H.F. Zhu, Y.Q. Huang, T. Okamura, X.H. Lu, Y. Song, G.X. Liu, W.Y. Sun, N. Ueyama, *Inorg. Chem.* 45 (2006) 8098.
- [13] J. Fan, W.Y. Sun, T. Okamura, W.X. Tang, N. Ueyama, *Inorg. Chem.* 42 (2003) 3168.
- [14] SIR92 A. Altomare, G. Cascarano, C. Giacovazzo, A. Guagliardi, M. Burla, G. Polidori, M. Camalli, *J. Appl. Crystallogr.* 27 (1994) 435.
- [15] P.T. Beurskens, G. Admiraal, G. Beurskens, W.P. Bosman, R. de Gelder, R. Israel, J.M.M. Smits, The DIRFID-99 Program System: Technical Report of the Crystallography Laboratory, University of Nijmegen, Nijmegen, The Netherlands, 1999.
- [16] CrystalStructure 3.8, Crystal Structure Analysis Package, Rigaku and Rigaku Americas, The Woodlands, TX, 2000–2007.
- [17] G.M. Sheldrick, SHELXS-97, Program for the Crystal Structure Solution, University of Göttingen, Göttingen, Germany, 1997.

- [18] SAINT, Program for Data Extraction and Reduction, Bruker AXS, Inc., Madison, WI, 2001.
- [19] G.M. Sheldrick, SADABS, University of Göttingen, Göttingen, Germany, 2000.
- [20] G.M. Sheldrick, SHELXTL, Version 6.10, Bruker Analytical X-Ray Systems, Madison, WI, 2001.
- [21] E. Barea, J.A.R. Navarro, J.M. Salas, N. Masciocchi, S. Galli, A. Sironi, Polyhedron 22 (2003) 3051.
- [22] W. Ouellette, A.V. Prosvirin, V. Chieffo, K.R. Dunbar, B. Hudson, J. Zubieta, Inorg. Chem. 45 (2006) 9346.
- [23] (a) V.A. Blatov, IUCr CompComm Newsl. 7 (2006) 4;
(b) V.A. Blatov, TOPOS, A Multipurpose Crystallochemical Analysis with the Program Package, Samara State University, Russia, 2009.
- [24] E.V. Alexandrov, V.A. Blatov, A.V. Kochetkov, D.M. Proserpio, CrystEngComm 13 (2011) 3947.
- [25] (a) B. Valeur, Molecular Fluorescence: Principles and Applications, Wiley-VCH, Weinheim, Germany, 2002;
(b) Y.Q. Huang, B. Ding, H.B. Song, B. Zhao, P. Ren, P. Cheng, H.G. Wang, D.Z. Liao, S.P. Yan, Chem. Commun. (2006) 4906.